Acta Crystallographica Section A
Foundations of Crystallography
ISSN 0108-7673

Received 24 February 2000
Accepted 9 October 2000

Electron crystallography without limits? Crystal structure of $Ti_{45}Se_{16}$ redetermined by electron diffraction structure analysis

Thomas E. Weirich†

Technische Universität Darmstadt, Fachbereich Material- und Geowissenschaften, Fachgebiet Strukturforschung, Petersenstrasse 23, D-64287 Darmstadt, Germany. Correspondence e-mail: weirich@gfe.rwth-aachen.de

The crystal structure of the metal-rich compound $Ti_{45}Se_{16}$ was redetermined from selected-area electron diffraction film data. The structure was solved by quasi-automatic direct methods using a data set of quantified *h*0*l* electron diffraction intensities. Improved atomic coordinates were obtained from a subsequent least-squares refinement on the basis of the kinematical approximation. The compound crystallizes in the monoclinic space group $C2/m$ with lattice parameters $a = 36.534$, $b = 3.453$, $c = 16.984$ Å, $\beta = 91.73^\circ$. The structure contains 23 titanium and 8 selenium atoms per asymmetric part of the unit cell. The refined atomic coordinates agree on average within 0.18 Å with the previously determined structure from high-resolution electron-microscopy images. The precision of the determined atomic coordinates obtained in this study is better than 0.05 Å. The structure of $Ti_{45}Se_{16}$ is the eighth metal-rich structure that has been solved by direct methods from two-dimensional selected-area electron diffraction data using the quasi-kinematical approximation. The present investigation proves again that direct methods with electron diffraction data work extremely reliably provided that the structure in question is composed of elements of nearly equal scattering power and that data covering the most significant parts of the unit-cell transform up to atomic resolution are available. Moreover, a method was developed that allows the estimation of the average crystal thickness from the effective atomic potential in the refined structure.

1. Introduction

In a recent study, it was shown that metal-rich inorganic crystal structures containing elements with atomic numbers between $Z = 16$ and 40 can be solved by quasi-automatic direct methods from single-crystal electron diffraction patterns using the kinematical approximation (Weirich *et al.*, 2000). According to this study, the most complex structures that have been solved from electron diffraction data are Ti_8Se_3 (Weirich *et al.*, 1996*b*) and $Ti_{11}Se_4$ (Weirich, Ramlau *et al.*, 1996), which contain 22 and 23 atoms per asymmetric unit. With the aim to check if the proposed method would be capable of solving structures of even higher structural complexity, a compound with 31 atoms per asymmetric unit, $Ti_{45}Se_{16}$, was chosen for the present investigation.

Besides the new phases β-Ti_2Se (Weirich *et al.*, 2000), Ti_8Se_3, $Ti_{11}Se_4$ and Ti_9Se_2 (Weirich Simon & Pöttgen, 1996), another previously unknown titanium selenide, $Ti_{45}Se_{16}$, was identified in the Ti–Se system (Weirich, Duppel *et al.*, 1996). The structure of $Ti_{45}Se_{16}$ was first solved by crystallographic image processing from high-resolution electron-microscopy (HREM) images. The structure contains 23 titanium and 8 selenium atoms per asymmetric part of the unit cell and crystallizes in the monoclinic space group $C2/m$ with approximate lattice parameters $a = 35.51$, $b = 3.45$, $c = 16.51$ Å, $\beta = 91.0^\circ$ (Weirich, 1996). In the following, the redetermination of the structure based on data from selected-area electron diffraction is reported.

2. Sample

High-temperature treatment of a sample with nominal composition Ti:Se of 8:3 yielded a multiphasic microcrystalline product. A small part of the earlier prepared sample was crushed in an agate mortar and microcrystals were collected on a carbon-film-supported copper grid. The sample was subsequently examined by transmission electron microscopy in a 300 kV JEOL 3010UHR microscope and a 200 kV Philips CM20UT microscope equipped with an HP-Ge detector for energy-dispersive X-ray spectroscopy (EDXS, Tracor Voyager). The electron-microscopy investigation revealed the

† Present address: Rheinisch-Westfälische Technische Hochschule Aachen, Central Facility for Electron Microscopy (Gemeinschaftslabor für Elektronenmikroskopie), Ahornstrasse 55, D-52074 Aachen, Germany.

presence of the phases α-Ti_2Se (Weirich *et al.*, 1996*a*), β-Ti_2Se and $Ti_{45}Se_{16}$ in the sample. Selected-area electron diffraction patterns from thin crystal areas were recorded at 300 kV on standard photographic EM film (Kodak SO-163 electron image film) and used in the course of the present structure determination.

3. Methods and results

The negatives were digitized by an 8 bit video-rate CCD camera (DAGE-MTI model CCD72E). Lattice parameters for a, c and the monoclinic angle β were determined from a calibrated electron diffraction pattern of $Ti_{45}Se_{16}$ recorded along the [010] direction. An electron diffraction pattern from the slightly off-axis tilted crystal was used for estimating the b axis (Fig. 1). However, a more accurate b parameter could be obtained from X-ray powder diffraction, which shows the common (020) peak for $Ti_{45}Se_{16}$ and β-Ti_2Se. The redetermined lattice parameters are $a = 36.534$, $b = 3.453$, $c = 16.984$ Å, $\beta = 91.73^\circ$. According to EDXS analysis of several crystallites, the compound contains 74 (2) at.% titanium and 26 (2) at.% selenium in good agreement with the assumed chemical composition.

Quantified electron diffraction intensities were extracted from a diffraction pattern of a $Ti_{45}Se_{16}$ crystallite which was aligned along the prominent [010] direction (Fig. 2*a*). The pattern was digitized in four partly overlapping sections, each containing 768 × 576 pixels. The image data were corrected for the non-linearity in the blackening curve and reflection intensities I_{hkl} in each of these four sections were estimated using the *ELD* program (Zou *et al.*, 1993). Merging the data on a fixed scale yielded a data set of 1047 crystallographically non-equivalent $h0l$ reflections with a resolution of about 0.6 Å. The internal R factor of symmetry-related reflections in the merged data set was only 11%, which confirms that the crystal was sufficiently well aligned along the [010] direction. Similar to the previous study (Weirich *et al.*, 2000), the data were phenomenological corrected for dynamical diffraction using the approximation $|F_{hkl}| \propto I_{hkl}$.

The structure was successfully solved in space group $C2/m$ using the direct-methods program *SIR97* (Altomare *et al.*, 1999), which was modified with scattering factors for electrons (Jiang & Li, 1984). The most probable solution obtained by *SIR97* had an R factor of 39.8%. All 122 atoms per unit cell

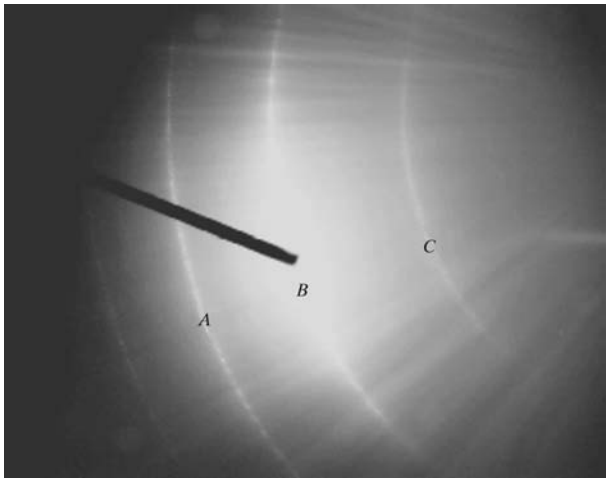

Figure 1
Electron diffraction pattern of a $Ti_{45}Se_{16}$ crystal which was tilted by about 9° from the [010] zone axis. The diffraction pattern shows the Laue cones of reflections (*A*) $h1l$, (*B*) $h0l$ and (*C*) $h,-1,l$ that have been used to determine the d spacing along the [010] direction (see Gard, 1976). The lattice parameter for the short b axis estimated from the radii of the cones is about 3.4 Å.

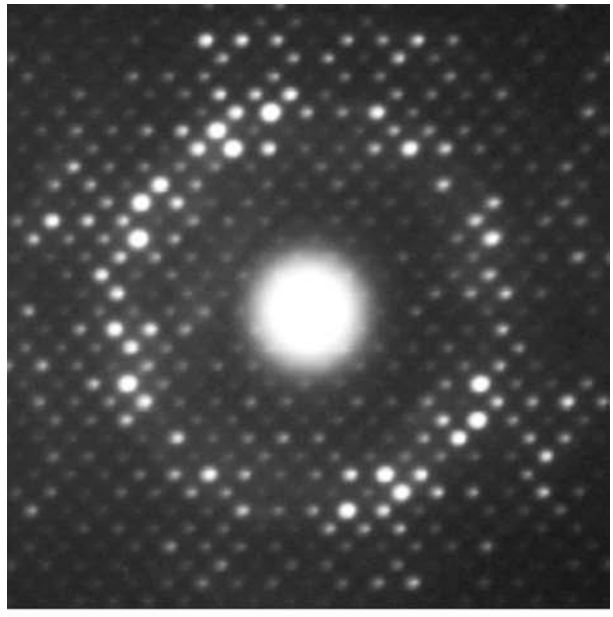

(*a*)

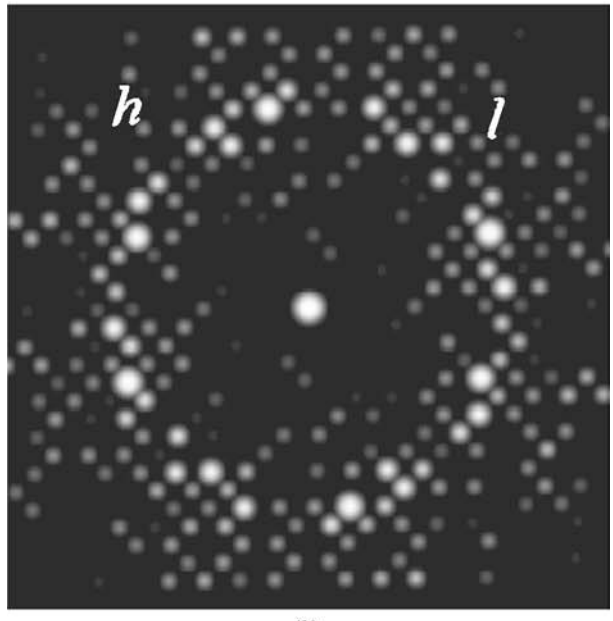

(*b*)

Figure 2
(*a*) Experimental selected-area electron diffraction pattern of $Ti_{45}Se_{16}$ recorded along the [010] direction (field limiting aperture 50 µm). (*b*) The kinematical electron diffraction pattern as calculated by the program *DIFPAT* (Skarnoulis *et al.*, 1979) using the atomic coordinates after least-squares structure refinement and assuming a crystal thickness of 100 Å.

were revealed in the potential map that was calculated from the 219 strongest ($h0l$) E values. Owing to the almost equal scattering power of the two atomic species, the assignment of the peaks to the corresponding atom type was performed manually using structural criteria instead of peak heights (for a more detailed discussion on the peak heights, see Appendix *A*). A structural model could readily be constructed from the obtained projected potential map since the basic building blocks in the substructure of these compounds are well known, *i.e.* the metal atoms form M_6 octahedral units and trigonal prisms around the non-metal atoms (Simon, 1981). Furthermore, these structures require that all atoms are located on mirror planes at heights of 1/2 or zero along the short axis. With this constraint, it was then possible to derive also the missing y coordinates for all atoms. In order to be consistent with the previous structure solution from HREM images, the origin of the unit cell was shifted according to $x' = x - 1/4$ and $z' = z - 1/2$. A subsequent least-squares structure refinement

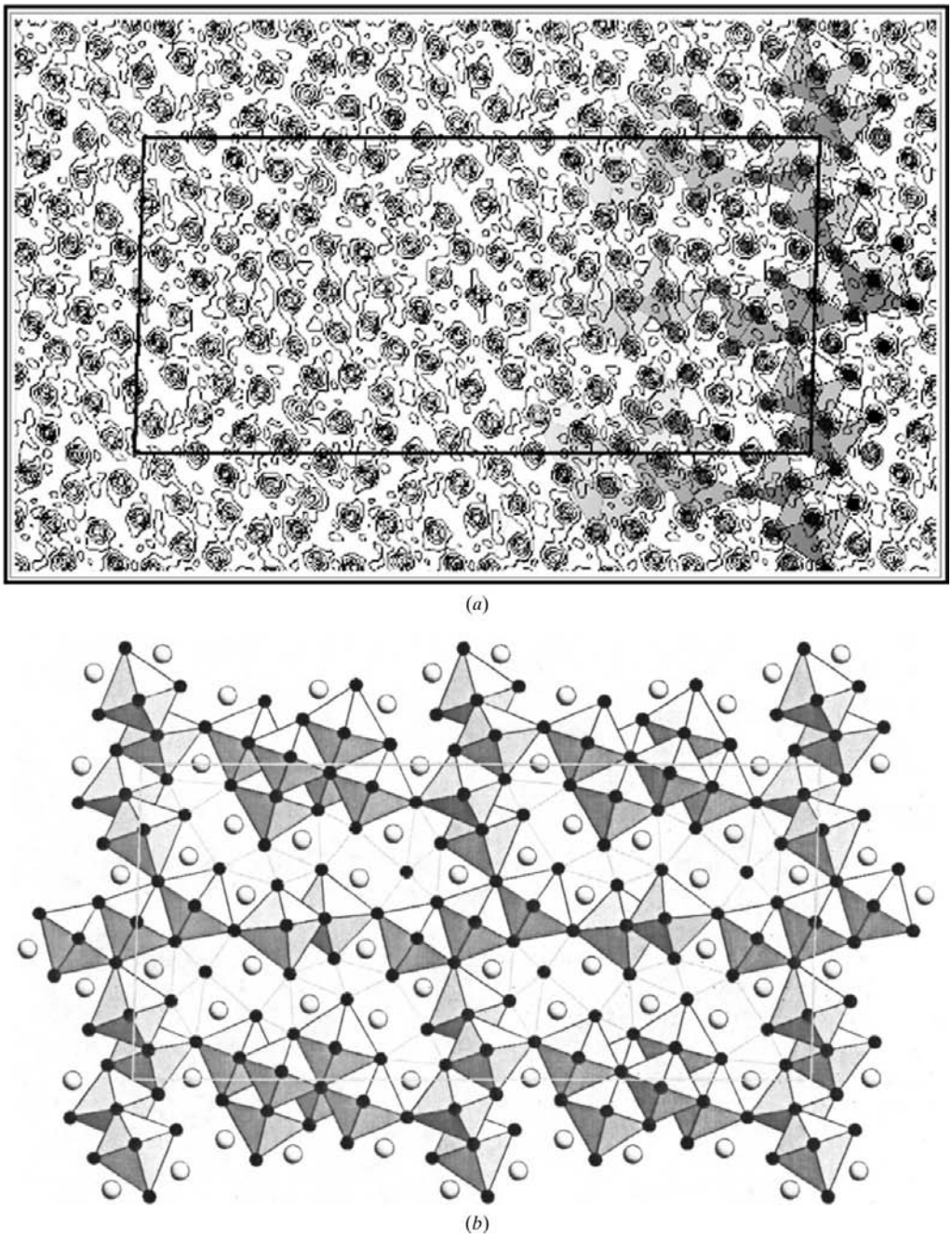

Figure 3
(*a*) Potential map for $Ti_{45}Se_{16}$ obtained by direct methods and least-squares structure refinement using the quantified $h0l$ electron diffraction data from the diffraction pattern in Fig. 2(*a*). The map shows the electrostatic potential distribution projected along the 3.453 Å axis. The peaks in the map were assigned to Ti atoms (black) and Se atoms (white), as indicated by the superimposed structural model on the right. (*b*) Complete structure model of $Ti_{45}Se_{16}$ after least-squares structure refinement. The Ti atoms form edge-sharing Ti_6 cluster units while all Se atoms are isolated inside the trigonal prisms of titanium.

Table 1
Refined atomic coordinates and atomic displacement factors of $Ti_{45}Se_{16}$.

Standard uncertainties are given in parentheses. The tabulated peak heights and atomic coordinates labelled DM refer to the structure solution obtained by *SIR97*. The corresponding coordinates labelled LS show the result after least-squares structure refinement with *SHELXL-97-2*. The *y* coordinates were derived using chemical criteria (see text).

	Peak height	*x* (DM)	*x* (LS)	*y*	*z* (DM)	*z* (LS)	U_{eq} (Å^2)
Ti1	430	0	0	0	1/2	1/2	0.027 (6)
Ti2	963	0.0262	0.0294 (6)	1/2	0.3679	0.3703 (13)	0.042 (6)
Ti3	429	0.9352	0.9426 (6)	1/2	0.4386	0.4376 (13)	0.042 (6)
Ti4	706	0.9154	0.9149 (3)	0	0.5512	0.5519 (7)	0.009 (3)
Ti5	506	0.8941	0.8966 (5)	0	0.3444	0.3409 (11)	0.033 (5)
Ti6	493	0.8537	0.8554 (6)	1/2	0.4722	0.4728 (13)	0.043 (6)
Ti7	1048	0.8801	0.8797 (7)	1/2	0.6684	0.6701 (15)	0.054 (7)
Ti8	534	0.7711	0.7712 (7)	1/2	0.3392	0.3338 (15)	0.056 (8)
Ti9	620	0.7938	0.7934 (6)	1/2	0.6172	0.6167 (12)	0.037 (5)
Ti10	619	0.7816	0.7782 (6)	0	0.4824	0.4890 (13)	0.045 (6)
Ti11	608	0.9478	0.9460 (6)	1/2	0.2495	0.2493 (12)	0.041 (6)
Ti12	599	0.0672	0.0665 (6)	1/2	0.1624	0.1593 (12)	0.039 (6)
Ti13	585	0.9786	0.9779 (6)	1/2	0.0952	0.0936 (12)	0.039 (6)
Ti14	575	0.0061	0.0066 (5)	0	0.2077	0.2058 (10)	0.027 (4)
Ti15	542	0.9060	0.9075 (7)	0	0.1175	0.1200 (15)	0.054 (8)
Ti16	515	0.9635	0.9621 (7)	0	0.9529	0.9536 (16)	0.063 (9)
Ti17	501	0.8198	0.8196 (6)	0	0.2015	0.2016 (13)	0.044 (6)
Ti18	1260	0.8414	0.8422 (4)	1/2	0.0685	0.0695 (9)	0.024 (4)
Ti19	755	0.8002	0.7990 (7)	1/2	0.8993	0.8996 (14)	0.048 (7)
Ti20	596	0.7815	0.7793 (5)	0	0.0225	0.0252 (10)	0.031 (5)
Ti21	750	0.8682	0.8666 (3)	0	0.9325	0.9350 (7)	0.011 (3)
Ti22	608	0.7379	0.7365 (9)	0	0.8627	0.8561 (19)	0.081 (12)
Ti23	625	0.8143	0.8139 (5)	0	0.7527	0.7454 (11)	0.033 (5)
Se1	940	0.7596	0.7592 (5)	1/2	0.7555	0.7617 (10)	0.045 (5)
Se2	828	0.8623	0.8605 (6)	1/2	0.8140	0.8092 (13)	0.062 (7)
Se3	584	0.9114	0.9115 (6)	1/2	0.0032	0.0039 (13)	0.060 (7)
Se4	373	0.8746	0.8754 (5)	1/2	0.2224	0.2186 (10)	0.041 (5)
Se5	489	0.8274	0.8272 (6)	0	0.3630	0.3616 (13)	0.063 (7)
Se6	726	0.8446	0.8397 (5)	0	0.5825	0.5855 (12)	0.049 (6)
Se7	703	0.9707	0.9735 (4)	0	0.3490	0.3499 (8)	0.024 (3)
Se8	623	0.0713	0.0739 (5)	0	0.2894	0.2908 (11)	0.050 (6)

carried out with the program *SHELXL97-2* (Sheldrick, 1998) yielded thermal displacement factors for all atoms that were of the same order as obtained in previous investigations (Weirich, Ramlau *et al.*, 1996; Weirich *et al.*, 1998, 2000). The overall *R* factor of the refined structure was 33% (92 parameters refined, unit weights). Since the intensities were not corrected for the curvature of the Ewald sphere, the obtained atomic displacement factors from least-squares refinement cover both the intensity decay due to the excitation error and the true thermal displacement. The refined atomic coordinates together with the initial atomic positions and peak heights of the structure solution are listed in Table 1. The *R* factors of the refinement at different resolution are listed in Table 2. It is interesting to note that the strongest reflections that appear between 3 and 1.5 Å agree much better with the refined model (*R* about 25%) than the very weak reflections at high resolution, which are much less affected by dynamical diffraction ($I_{hkl} \propto |F_{hkl}|^2$). The average positional shift of the atoms during the refinement was 0.08 Å (maximum shift 0.27 Å for Ti3). The obtained standard deviations for the refined atom positions range from 0.016 to 0.046 Å. The difference between the previous structure solution from HREM images and the refined atomic coordinates based on the electron diffraction data is on average 0.18 Å (maximum deviation 0.46 Å for Ti15). The obtained potential map after least-squares refinement and the complete structural model for $Ti_{45}Se_{16}$ are shown in Figs. 3(*a*) and 3(*b*).

A sensitive test for the correctness of the refined structure is provided by the shortest Ti—Se distances within the trigonal prisms. These range for the present structure from 2.5 to 2.7 Å, in good agreement with the calculated distances for the other titanium selenide structures that contain the same structural unit. Furthermore, the good quality of the refined structure model is also realized by comparing the experimental and the calculated (kinematical) electron diffraction patterns in Figs. 2(*a*) and 2(*b*).

4. Discussion

The structure of $Ti_{45}Se_{16}$ is at present the eighth in a line of metal-rich structures that have been solved by quasi-automatic direct methods from two-dimensional selected-area electron diffraction data (Weirich *et al.*, 1998, 2000). Among these compounds, $Ti_{45}Se_{16}$ has the most complex structure with 31 unique atoms followed by the structures of Ti_8Se_3 and $Ti_{11}Se_4$, which contain 22 and 23 atoms per asymmetric unit. However, the fact that very complex structures such as $Ti_{45}Se_{16}$, Ti_8Se_3 and $Ti_{11}Se_4$ can be solved and refined from standard electron diffraction data is in striking contradiction to the until recently held doubts of this approach in general (Williams & Carter, 1996). With the aim to clear this inconsistency, the present author wants to focus on the boundary conditions that facilitated the use of the quasi-kinematical approximation, which worked so amazingly well for this class of metal-rich compounds.

According to Dorset (1999), one has a fair chance to solve a structure by direct phasing techniques from electron data if 'reflections from the most significant parts of the unit cell transform can be measured and the experimental Patterson function is well correlated to the autocorrelation function of the actual structure'. Whitfield *et al.* (1999) use Sayre's theorem (Sayre, 1952) to explain why the quasi-kinematical approach holds in some cases. These authors stress that a structure consisting of non-overlapping peaks of (nearly) equal weight can be *squared* without changing the geometric part of the structure factor. Even if the shape of the atomic scattering factor has become unphysical by squaring the structure factors, the structure can still be solved (and refined) from such modified data since the positions of the atomic peaks remain unchanged. These arguments reasonably explain

Table 2
R factors for the structure refinement of $Ti_{45}Se_{16}$ at different crystallographic resolution.

Each resolution range contains about 103 to 106 unique reflections from electron diffraction.

Resolution range (Å)			*R* factor (%)
18.26	–	2.14	24.8
2.14	–	1.52	24.8
1.52	–	1.24	27.7
1.24	–	1.07	29.7
1.07	–	0.97	39.3
0.97	–	0.88	39.6
0.88	–	0.81	43.9
0.81	–	0.74	49.9
0.74	–	0.68	58.6
0.68	–	0.62	67.8

why $Ti_{45}Se_{16}$ and its related structures could be solved by direct methods from single projection data. All these structures have in common that the atomic species have an almost identical electrostatic potential and that there exists a projection with non-overlapping atomic columns along one principal axis. Moreover, about 50% of all theoretically accessible reflections for these structures can be obtained from a single diffraction pattern which is recorded along the prominent short crystal axis. This necessarily means that the most significant part of the unit-cell transform is always covered by such data (see the argument given by Dorset). How robust direct methods work with such projected data is demonstrated by another example, the structure of α-V_4As_4 (Yvon & Boller, 1972), which was solved from data of a diffraction pattern (Fig. 4*a*) that was digitized directly from the published article (Andersson *et al.*, 1976). The structure solution for α-V_4As_4 suggested by *SIR97* had an *R* factor of 31%. Again, all atoms could be located in the received potential map projected along the short *a* axis. Two-dimensional atom positions (*y* and *z*) were obtained from the map and a new potential map (Fig. 4*b*) was calculated from the 26 strongest *E* values, which revealed all atom positions by separated sharp peaks. The atomic coordinates obtained from the initial map were within 0.51 Å of the published X-ray structure shown in Fig. 4(*d*). The average deviation between the two structural models is 0.18 Å.

In a previous study (Weirich *et al.*, 2000), it was shown for a medium–thick crystallite of Ti_9Se_2 that dynamical diffraction coupled with secondary scattering 'decreases the intensity of the strong reflections and increases the intensity of weak reflections so that the intensity distribution becomes more even' (Cowley, 1953). For medium–thick crystals (approximately 50–150 Å for the titanium selenides investigated here), the difference between the strong and the weak intensities does not vanish completely such that the strong reflections are still kept among the highest ranked *E* values after normalizing the data, which is most important for the success of direct methods. According to dynamical theory (Bethe, 1928; MacGillavry, 1940; Pinsker, 1953; James, 1965) and from experiment (Blackman, 1939), it is known that the intensity of the diffracted beams I_{hkl} becomes proportional to $|F_{hkl}|$ for thick crystals. Hence the approximation $|F_{hkl}| \propto I_{hkl}$ appears most adequate for precompensating dynamical effects in the early stages of a structure determination of unknowns as demonstrated also by others (Nicolopoulos *et al.*, 1995). Unlike Sayre's theorem, the above phenomenological compensation for dynamical diffraction is equivalent to *rooting* the structure instead of squaring it. In this context, it is interesting to note that the square root of the structure-factor amplitude has also been suggested for phase extension (Davies & Rollett, 1976). An important benefit from the above approximation is that standard programs from X-ray crystallography can be used to refine the structure. Incorporating *n*-beam dynamical calculations at this stage of a structure determination is at the present state impossible for data from selected-area electron diffraction because this technique unavoidably accumulates the scattering from crystal areas of varying thickness (see Appendix *A*). Since crystal thickness is an important parameter when dynamical diffraction is considered, *e.g.* by the structure refinement program *MSLS* (Jansen *et al.*, 1998), data from electron microdiffraction are required to ensure that the recorded intensities are collected from a crystal area of (almost) constant thickness. However, that quasi-kinematical structure refinements using two-dimensional data from selected-area electron diffraction are justified under certain conditions has been repeatedly shown (Weirich, Ramlau *et al.*, 1996; Weirich *et al.*, 1998, 2000). Although the *R* factor of the refined structure can vary up to 40%, *e.g.* as determined for Zr_2Se, the result might still be correct within 0.05 Å for the heavy-atom positions (Weirich, 1998). This dilemma forces us to search for other criteria than *R* factors to prove the correctness of a structure. Atom distances and bond angles, for example, as used in the present case are good alternatives since their quantities can easily be compared with those from structurally related compounds. This requires, however, that the unit-cell dimensions have been accurately determined from electron-microscopy data. Another independent alternative to check the correctness of a structure is provided by quantum-mechanical calculations from first principles. Once a rough structure model has been established, these calculations allow the structure to relax to its energetic minimum, *i.e.* finding optimized atomic positions and lattice parameters (Winkler, 1999). The main disadvantage of this approach, on the other hand, is the enormous computing times required (up to several days) to perform these calculations for larger structures.

5. Conclusions

The quasi-kinematical approach has been used to determine, *i.e.* solve, and refine the metal-rich structure $Ti_{45}Se_{16}$, which contains 31 atoms in the asymmetric part of the unit cell. The good geometry of the refined structure model and the close resemblance of the experimental and calculated kinematical electron diffraction patterns verifies the method used for determining the structure. The main boundary conditions that supported successfully employing the quasi-kinematical approach were that the compound is composed of elements

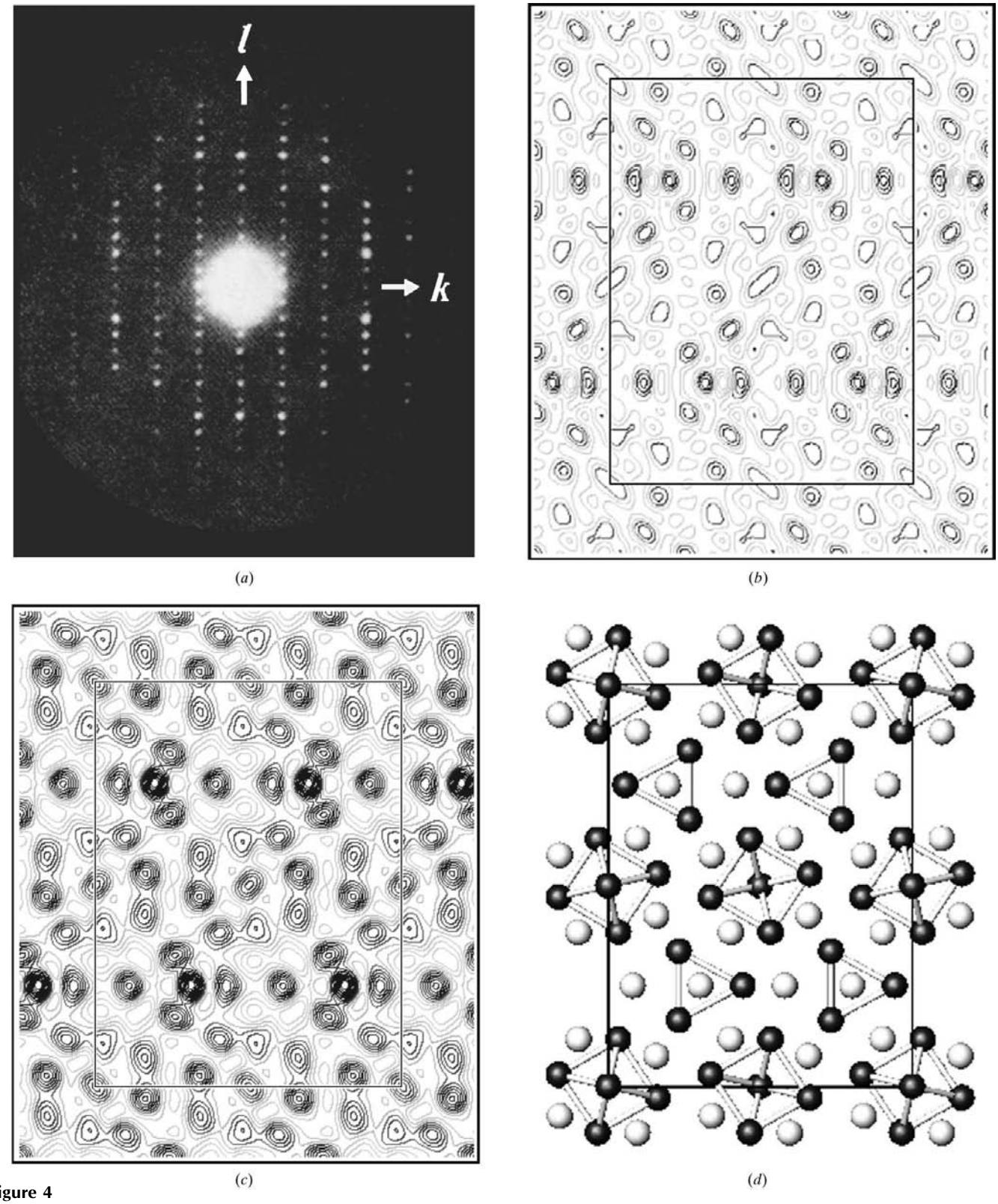

Figure 4
(*a*) Experimental selected-area electron diffraction pattern of α-V_4As_3 recorded along the short *a* axis. The image was obtained by digitizing the diffraction pattern from the article by Andersson *et al.* (1976). [Reproduction with kind permission by Academic Press Inc.] Processing of the diffraction pattern yielded 79 unique reflections with a crystallographic resolution of 1.1 Å which were subsequently used as input for the direct-methods program *SIR97*. (*b*) Potential map from the 26 strongest (0*kl*) *E* values with phases calculated from the atomic coordinates obtained by the structure solution. The map shows all atom positions correct within 0.51 Å to the X-ray structure in (*d*). (*c*) Potential map as in (*b*) but calculated with all 79 observed (0*kl*) structure-factor amplitudes. (*d*) Structure model of α-V_4As_3 in projection along the short *a* axis as obtained from X-ray crystallography (Yvon & Boller, 1972). The structure crystallizes in space group *Cmcm* with lattice parameters $a = 3.420$, $b = 13.730$, $c = 18.120$ Å. The vanadium atoms (black) form strings of apex-linked V_6 octahedra and trigonal prisms around the arsenic atoms (white).

that have an almost identical electrostatic potential and that data (at least from one orientation) could be obtained that allowed the atom columns to be resolved in projection. Moreover, it was shown that these conditions favour also refinement of the structure by standard programs from X-ray crystallography. Despite some existing limits to refine any structure with data from electron microscopy on the kinematical assumption, this approach has yielded up to now good refinement results for the heavy-atom structures $Ti_{11}Se_4$, β-Ti_2Se and $Ti_{45}Se_{16}$. In the case of the structurally related compounds Zr_2Se (Weirich, 1998) and Ta_2P (Weirich *et al.*, 1998), however, only the heavier atoms could be refined with high accuracy while the selenium positions could not be refined and the phosphorous could not be detected.

Structures that have no short crystal axis and/or no projection with non-overlapping atom columns require collection of three-dimensional data for solving the structure. This is a very demanding task since intensities from several zone axes that have been differently affected by dynamical scattering must be merged together to yield a single data set. Nevertheless, although such data are expected to be only rough estimates of the correct intensities, it turns out in practice that the obtained quality is often sufficient to solve and to complete the structural model. That this approach works reasonably well was demonstrated by the recent structure determinations of Al_mFe (Gjønnes *et al.*, 1998), Nd_2CuO_4 (Bougerol-Chaillout *et al.*, 1999) and ϕ-$Bi_8Pb_5O_{17}$ (Gemmi *et al.*, 2000).

In view of the very complex structures that have been solved so far from electron-microscopy data, one is tempted to seek the limits of the approximations made as has been tried with the present work. It is of course not possible to give a clear answer in advance whether a structure can be solved using the quasi-kinematical approximation or not. However, it is evident from practical work that there are (sometimes strict) limitations that prevent determination of structures from scratch using electron diffraction data. In particular, data corruption by dynamical diffraction is difficult to estimate (and to treat) in the initial stages of an *ab initio* structure determination of unknowns. This often requires application of empirical corrections as in the present case in order to arrive at the correct structure solution. Although the simple kinematical approach was extremely successful in the case of the discussed metal-rich structures, the present author is aware of the fact that this approach might not work with similar reliability despite all efforts that have perhaps been undertaken to collect the best *kinematical* data, *e.g.* from thin crystallites. On the other hand, the increasing number of successful structure determinations that have been reported during the last few years using electron-microscopy images, convergent-beam electron diffraction, electron microdiffraction and selected-area electron diffraction prove that many of the anticipated limits for electron crystallography could be overcome in practice, much to the contrary of the pessimistic predictions from earlier theory (Claffey *et al.*, 1970; Cowley, 1993, Eades, 1994; Sturkey, 1977). Thus, the obtained progress in determining structures from electron diffraction data supports strongly what the Russian inventors of electron crystallography, Professors Z. G. Pinsker and B. K. Vainshtein stated in the 1950's and what might also be a suitable answer to the question raised in the title: 'Structure analysis by electron diffraction must be regarded as an independent method for determining the atomic structure of matter and, as such, is finding an ever-widening field of application' (Vainshtein, 1964).

APPENDIX *A*

One of the problems in determining crystal structures from selected-area electron diffraction data arises from the morphology of the specimen. While a perfect crystal for structure determination is thin and of constant thickness, real crystallites are often irregular and wedge shaped. Data collection from such a specimen, even when only the thinnest parts have been used, are always an average over a certain thickness range. In order to look closer at this effect, a series of exit-wave functions was calculated for $Ti_{45}Se_{16}$ by a standard program for HREM image simulation (Kilaas & O'Keefe, 1997). These calculations were performed for crystal thicknesses between 5 and 150 Å using a step width of 5 Å. A subsequent quantitative analysis of the received effective potential maps shows that the Se:Ti potential ratio stays nearly constant between 5 and 30 Å (Fig. 5). With increasing crystal thickness, the potential ratio declines rapidly until about 110 to 115 Å where the selenium potential is zero. As a result, the scattering of the crystal is fully dominated by the titanium framework at this minimum (Fig. 6*c*). The crossover on the left side of the minimum, where titanium and selenium have the same effective potential, corresponds to a crystal thickness of about 60 Å (Fig. 6*b*). Beyond the minimum, the effective potential of selenium is recovered until the potential of titanium has now vanished totally at about 150 Å. The principal difficulty to correlate data from selected-area electron diffraction with crystal thickness (which is an indispensable

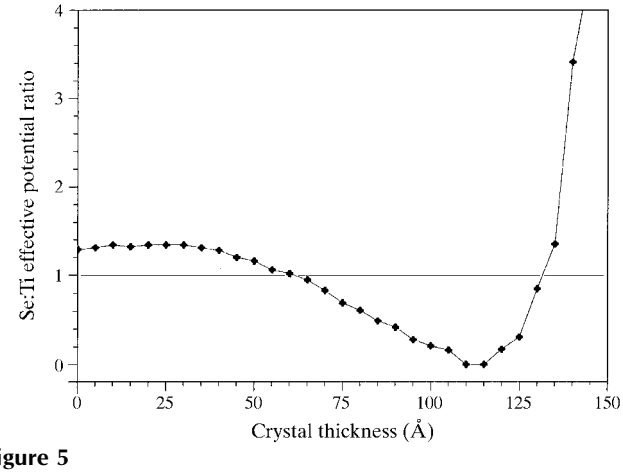

Figure 5
Trace of the effective Se:Ti potential ratio *versus* crystal thickness for $Ti_{45}Se_{16}$ as obtained from calculated exit-wave maps (see text). The ratio at zero thickness was determined from the projected potential map calculated for one unit cell.

precondition for correcting dynamical effects!) is immediately seen from the former analysis. Owing to this averaging effect, difficulties arise also to assign the correct atomic species to the peak heights in the initial potential maps obtained from direct methods if the topology of the structural fragments is unknown. Nevertheless, it seems possible to use these maps for estimating the average crystal thickness from the peak heights of the refined structure. The average Se:Ti ratio in the potential map for $Ti_{45}Se_{16}$ after refinement is close to 1.0 with an estimated error of about 0.2. According to the plot shown in Fig. 5, this value is equal to an effective average crystal thickness of about 60 Å. Assuming an ideal wedge-shaped crystal (45° angle of gradient up and down) and taking the scattering volume into account means that the above value would correspond to a thickness range between zero and about 84 Å. This thickness is only somewhat lower than that used for calculating the kinematical diffraction pattern in Fig. 2(*b*). With further improvements, *e.g.* determining more accurate intensities from a slow-scan CCD camera or from an imaging plate, this method might be an alternative method for estimating the average thickness of the specimen, a parameter that often remains unknown in this type of investigation.

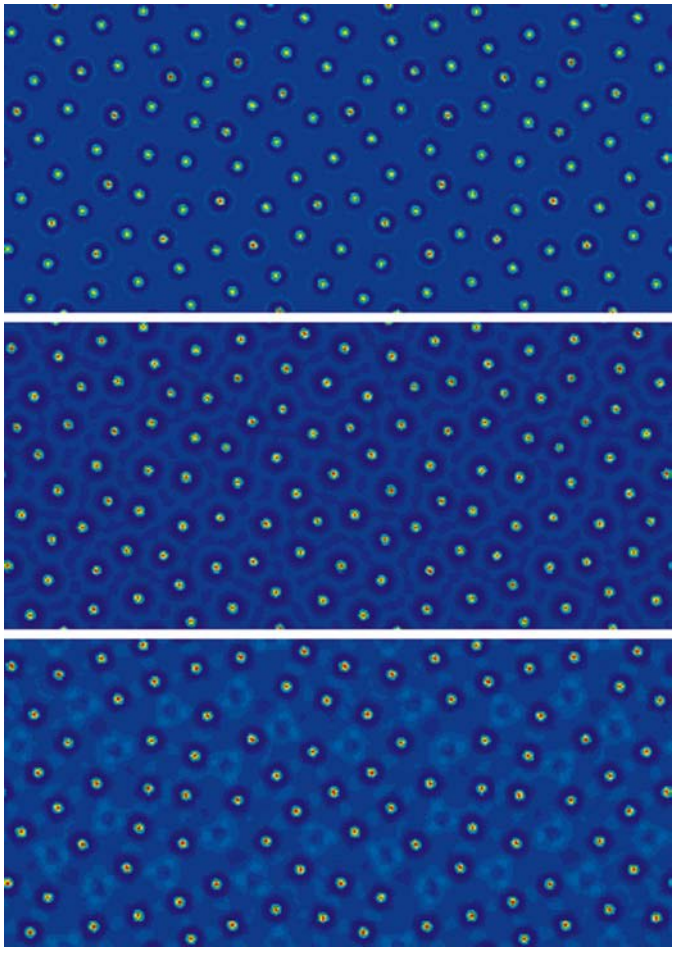

Figure 6
Calculated exit-wave potential maps along the [010] direction for $Ti_{45}Se_{16}$ using the *NCEMSS* program (Kilaas & O'Keefe, 1997). According to the plot shown in Fig. 5, the selenium atoms have a significantly higher potential than the titanium atoms when the crystal is thin, *e.g.* 25 Å (potential map at the top). With increasing crystal thickness, the effective potential of the selenium atoms declines until it becomes equal to that of titanium at a crystal thickness of about 60 Å (middle). If the crystal gets thicker, the effective potential of the selenium atoms falls below that of the titanium atoms until its contribution vanishes entirely at about 110 Å (bottom).

References

Altomare, A., Burla, M. C., Camalli, M., Cascarano, G., Giacovazzo, C., Guagliardi, A., Moliterni, A. G. G., Polidori, G. & Spagna, R. (1999). *J. Appl. Cryst.* **32**, 115–118.

Andersson, S., Annehed, H., Stenberg, L. & Berger, R. (1976). *J. Solid State Chem.* **19**, 170–173.

Bethe, H. (1928). *Ann. Phys. (Leipzig)*, **87**, 55–129.

Blackman, M. (1939). *Proc. R. Soc. London Ser. A*, **173**, 68–82.

Bougerol-Chaillout, C., Tranqui, D., Gemmi, M., Migliori, A. & Calestani, G. (1999). *Acta Cryst.* A**55** Supplement, Abstract P12.02.033.

Claffey, W. J., Priore, R. & Parsons, D. F. (1970). *J. Appl. Cryst.* **3**, 516–519.

Cowley, J. M. (1953). *Acta Cryst.* **6**, 516–521.

Cowley, J. M. (1993). *International Tables for Crystallography*, Vol. B, edited by U. Shmueli, p. 280. Dordrecht: Kluwer Academic Publishers.

Davies, A. R. & Rollett, J. S. (1976). *Acta Cryst.* A**32**, 17–23.

Dorset, D. L. (1999). *Acta Cryst.* A**55** Supplement, Abstract M05.BB.002.

Eades, J. A. (1994). *Acta Cryst.* A**50**, 292–295.

Gard, J. A. (1976). *Electron Microscopy in Mineralogy*, edited by H. R. Wenk, p. 54. Berlin: Springer Verlag.

Gemmi, M., Righi, L., Calestani, G., Migliori, A., Speghini, A., Santarosa, M. & Bettinelli, M. (2000). *Ultramicroscopy*, **84** 133–142.

Gjønnes, J., Hansen, V., Berg, B. S., Runde, P., Cheng, Y. F., Gjønnes, K., Dorset D. L. & Gilmore, C. J. (1998). *Acta Cryst.* A**54**, 306–319.

James, R. W. (1965). *The Optical Principles of the Diffraction of X-rays*, pp. 59–60. London: G. Bell and Sons.

Jansen, J., Tang, D., Zandbergen, H. W. & Schenk, H. (1998). *Acta Cryst.* A**54**, 91–101.

Jiang, J. S. & Li, F. H. (1984). *Acta Phys. Sin.* **33**, 845–849.

Kilaas, R. & O'Keefe, M. A. (1997). *NCEMSS – Program for the Simulation of HRTEM Images.* Linux version 1.6. National Center for Electron Microscopy, Materials Science Division, Lawrence Berkeley Laboratory, University of California, Berkeley, USA.

MacGillavry, C. H. (1940). *Physica (Utrecht)*, **7**, 329–343.

Nicolopoulos, S., Gonzales-Calbet, J. M., Vallet-Regi, M., Corma, A., Corell, C., Guil, J. M. & Perez-Pariente, J. (1995). *J. Am. Chem. Soc.* **117**, 8947–8956.

Pinsker, Z. G. (1953). *Electron Diffraction*, pp. 179–180. London: Butterworths.

Sayre, D. (1952). *Acta Cryst.* **5**, 60–65.

Sheldrick, G. M. (1998). *SHELXL-97–2. Program for Crystal Structure Refinement.* University of Göttingen, Germany.

Simon, A. (1981). *Angew. Chem. Int. Ed. Engl.* **20**, 1–22.

Skarnoulis, A. J., Liljestrand, L. & Kihlborg, L. (1979). *Chem. Commun.* **1**, 1–27.

Sturkey, L. (1977). *Trans. Am. Crystallogr. Assoc.* **13,** 1–13.

Vainshtein, B. K. (1964). *Structure Analysis by Electron Diffraction.* Oxford: Pergamon Press.

Weirich, T. E. (1996). PhD thesis, Universität Osnabrück, Germany.

Weirich, T. E. (1998). Unpublished results.

Weirich, T. E., Duppel, V., Ramlau R. & Simon, A. (1996). Unpublished results.

Weirich, T. E., Hovmöller, S., Kalpen, H., Ramlau, R. & Simon, A. (1998). *Crystallogr. Rep.* **43**, 956–967.

Weirich, T. E., Pöttgen, R. & Simon, A. (1996*a*). *Z. Kristallogr.* **212**, 928.

Weirich, T. E., Pöttgen, R. & Simon, A. (1996*b*). *Z. Kristallogr.* **212**, 929–930.
Weirich, T. E., Ramlau, R., Simon, A., Hovmöller, S. & Zou, X. D. (1996). *Nature (London)*, **382**, 144–146.
Weirich, T. E., Simon, A. & Pöttgen, R. (1996). *Z. Anorg. Allg. Chem.* **622**, 630–634.
Weirich, T. E., Zou, X. D., Ramlau, R., Simon, A., Cascarano, G. L., Giacovazzo, C. & Hovmöller, S. (2000). *Acta Cryst.* A**56**, 29–35.
Whitfield, H. J., Moodie, A. F., Etheridge, J. & Humphreys, C. J. (1999). *Acta Cryst.* A**55** Supplement, Abstract P05.BB.004.
Williams, D. B. & Carter, C. B. (1996). *Transmission Electron Microscopy*, Vol. 2, p. 203. New York: Plenum Press.
Winkler, B. (1999). *Z. Kristallogr.* **214**, 506–527.
Yvon, K. & Boller, H. (1972). *Monatsh. Chem.* **103**, 1643–1650.
Zou, X. D., Sukharev, Y. & Hovmöller, S. (1993). *Ultramicroscopy*, **52**, 436–444.